PHYSICAL REVIEW B **87**, 121401(R) (2013)

Metal-insulator transition and phase separation in doped AA-stacked graphene bilayer

A. O. Sboychakov,[1,2] A. L. Rakhmanov,[1,2,3] A. V. Rozhkov,[1,2] and Franco Nori[1,4]

[1]*Advanced Science Institute, RIKEN, Wako-shi, Saitama, 351-0198, Japan*

[2]*Institute for Theoretical and Applied Electrodynamics, Russian Academy of Sciences, 125412 Moscow, Russia*

[3]*Moscow Institute for Physics and Technology (State University), 141700 Moscow Region, Russia*

[4]*Department of Physics, University of Michigan, Ann Arbor, Michigan 48109-1040, USA*

(Received 21 October 2012; published 4 March 2013)

We investigate the doping of AA-stacked graphene bilayers. By applying a mean field theory at zero temperature we find that, at half-filling, the bilayer is an antiferromagnetic insulator. Upon doping, the homogeneous phase becomes unstable with respect to phase separation. The separated phases are undoped antiferromagnetic insulator and metal with a nonzero concentration of charge carriers. At sufficiently high doping, the insulating areas shrink and disappear, and the system becomes a homogeneous metal. The conductivity changes drastically upon doping, so the bilayer may be used as a switch in electronic devices. The effects of finite temperature are also discussed.

DOI: 10.1103/PhysRevB.87.121401 PACS number(s): 73.22.Pr, 73.22.Gk, 73.21.Ac

Introduction. Controlled metal-insulator (M-I) transitions are very useful for electronic applications of graphene.[1] Such transitions have been analyzed theoretically (e.g., Ref. 2) and experimentally observed in graphene by several groups using different techniques, e.g., chemical adsorption,[3] thermal annealing,[4] gate-induced M-I transition,[5] and percolation-driven M-I transition in graphene nanoribbons due to inhomogeneous electron-hole puddle formation.[6]

Here we study an AA-stacked bilayer of graphene (AA-BLG). The purpose of this work is to demonstrate that this system, which has been successfully fabricated recently,[7,8] can exhibit a M-I transition upon doping. Further, we demonstrate that the required levels of doping are within current experimental capabilities. Unlike AB-stacked bilayers, the AA-BLG received very modest theoretical attention.[8–13] However, advances in fabrication of AA-stacked bilayers and multilayers[7,8] underscore the need for thorough theoretical investigations.

Tight-binding calculations for AA-BLG[9,10] predict that near the Fermi energy the bilayer has two bands, one electron-like and one hole-like. These bands have Fermi surfaces, unlike Fermi points in monolayer graphene and AB-stacked bilayers. An important feature of the AA-BLG is that the hole and electron Fermi surfaces coincide. As shown in Ref. 13, if interactions are included, these degenerate Fermi surfaces become unstable, and the bilayer turns into an antiferromagnetic (AFM) insulator with a finite gap. This electronic instability is strongest when the bands cross at the Fermi energy. Impurities or doping shift the Fermi level and suppress the AFM instability.

Superficially, one may expect that the AFM gap Δ decreases with doping x and vanishes above some critical value x_c. However, we show that the homogeneously doped state is unstable with respect to the phase separation into undoped AFM insulator and doped metal. As the doping grows, the concentration of the AFM insulator shrinks, while it grows for the metal. Above a certain threshold x^*, metallic islands connect into an infinite cluster and the percolation-driven insulator-metal transition occurs, at which point the sample becomes metallic.

Here we study the electronic properties of the doped AA-BLG in the framework of the Hubbard-like model used in Ref. 13. We determine how the gap Δ depends on x in the homogeneous state and find the critical value x_c, where Δ vanishes. We further show that at small doping the homogeneous state is unstable because the compressibility of the system is negative and find the doping range where this instability arises. The effects of nonzero temperature are also discussed.

The model. The Hamiltonian for p_z electrons of carbon atoms for the AA-BLG can be written as

$$H = H_0 + H_{\rm int} - \mu\hat{N}, \tag{1}$$

where H_0 describes electron hopping, $H_{\rm int}$ is the electron-electron interaction, μ is the chemical potential, and $\hat{N}$ is the operator of the total electron number in the system. In the tight-binging approximation

$$H_0 = -t\sum_{\langle \mathbf{nm}\rangle i\sigma} a^\dagger_{\mathbf{n}i\sigma} b_{\mathbf{m}i\sigma} - t_0\left(\sum_{\mathbf{n}\sigma} a^\dagger_{\mathbf{n}1\sigma} a_{\mathbf{n}2\sigma} + \sum_{\mathbf{m}\sigma} b^\dagger_{\mathbf{m}1\sigma} b_{\mathbf{m}2\sigma}\right) + \text{H.c.} \tag{2}$$

Here $a^\dagger_{\mathbf{n}i\sigma}$ and $a_{\mathbf{n}i\sigma}$ ($b^\dagger_{\mathbf{m}i\sigma}$ and $b_{\mathbf{m}i\sigma}$) are the creation and annihilation operators of an electron with spin σ in the layer $i = 1, 2$ on the sublattice $\mathcal{A}$ ($\mathcal{B}$) at site $\mathbf{n} \in \mathcal{A}$ ($\mathbf{m} \in \mathcal{B}$). The amplitude t (t_0) in Eq. (2) describes the in-plane (interplane) nearest-neighbor hopping. For calculations we use the values of the hopping integrals $t \approx 2.57$ eV, $t_0 \approx 0.36$ eV specific to multilayer AA systems.[14] Longer-range hoppings are neglected because these are small (about or less than 0.1 eV), and we checked that the effects they produce are negligible (within 1–2%).

The onsite Coulomb interaction can be written as

$$H_{\rm int} = \frac{U}{2}\sum_{\mathbf{n}i\sigma}\left(n_{\mathbf{n}i\mathcal{A}\sigma} - \frac{1}{2}\right)\left(n_{\mathbf{n}i\mathcal{A}\bar{\sigma}} - \frac{1}{2}\right) + \frac{U}{2}\sum_{\mathbf{m}i\sigma}\left(n_{\mathbf{m}i\mathcal{B}\sigma} - \frac{1}{2}\right)\left(n_{\mathbf{m}i\mathcal{B}\bar{\sigma}} - \frac{1}{2}\right), \tag{3}$$

where $n_{\mathbf{n}i\mathcal{A}\sigma} = a^\dagger_{\mathbf{n}i\sigma} a_{\mathbf{n}i\sigma}$, $n_{\mathbf{m}i\mathcal{B}\sigma} = b^\dagger_{\mathbf{m}i\sigma} b_{\mathbf{m}i\sigma}$, and $\bar{\sigma} = -\sigma$. It is known that the onsite Coulomb interaction in graphene

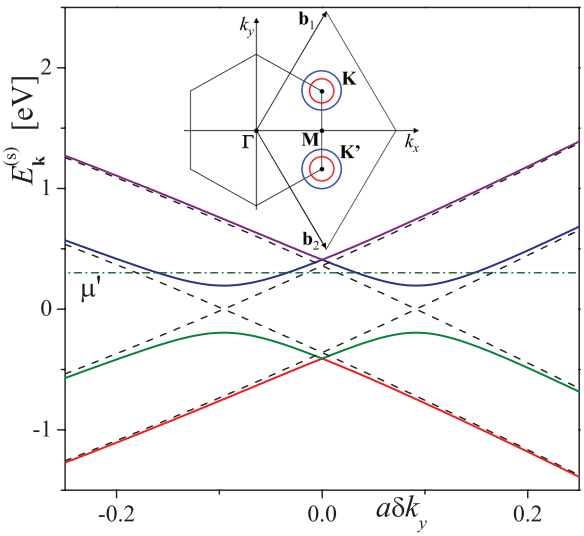

FIG. 1. (Color online) The band structure for the homogeneous phase of the AA-stacked bilayer graphene near the **K** point; $\mathbf{k} = \mathbf{K} + \delta k_y \mathbf{e}_y$. The dashed lines show the noninteracting single-electron bands. At half filling these bands intersect with each other at the Fermi energy $\mu = 0$. Adding interactions opens a gap. The mean field bands [see Eqs. (7)] are shown by solid lines. With doping, these bands are filled up to the level $\mu' = \mu - Ux/2$. As a result of doping, the Fermi surface degeneracy disappears, and we have two Fermi surface components around each Dirac point. The inset shows the first Brillouin zone (hexagon) and the reciprocal lattice unit cell (rhombus) of the AA-BLG. Circles around the **K** and **K**′ points correspond to Fermi surfaces of the doped system.

and other carbon systems is rather strong, but the estimates available in the literature vary considerably,[15,16] ranging from $U \sim t$ to $\sim 4t$. Because of this uncertainty, we present our results in the form of U-dependent functions rather than definite estimates.

Antiferromagnetic state. In the absence of electron-electron coupling, $U = 0$, and zero doping ($x = 0$, which corresponds to half filling) the AA-BLG band structure is shown in Fig. 1 by dashed lines. Two bands pass through the Fermi energy level near the Dirac points $\mathbf{K} = 2\pi\{\sqrt{3}, 1\}/(3\sqrt{3}a)$ and $\mathbf{K}' = 2\pi\{\sqrt{3}, -1\}/(3\sqrt{3}a)$, where a is the in-plane carbon-carbon distance. The chemical potential is $\mu = 0$, while the Fermi surfaces are given by the equation $|f_{\mathbf{k}}| = t_0/t$, where

$$f_{\mathbf{k}} = 1 + 2\exp(3ik_x a/2)\cos(k_y a\sqrt{3}/2). \tag{4}$$

For $t_0/t \ll 1$, one can expand the function $|f_{\mathbf{k}}|$ near the Dirac points and demonstrate that the Fermi surface consists of two circles with radius $k_r = 2t_0/(3ta)$ around the Dirac cones **K** and **K**′. Upon doping, these Fermi surfaces are transformed into four circles [see the inset in Fig. 1]. The presence of two bands with identical Fermi surfaces makes the system unstable with respect to spontaneous symmetry breaking.

Since the unit cell of AA-BLG consists of four atoms, it is convenient to introduce the bispinors $\psi^\dagger_{\mathbf{k}\sigma} = (\psi^\dagger_{\mathbf{k}\mathcal{A}\sigma}, \psi^\dagger_{\mathbf{k}\mathcal{B}\sigma})$, with spinor components $\psi^\dagger_{\mathbf{k}\mathcal{A}\sigma} = (a^\dagger_{\mathbf{k}1\sigma}, a^\dagger_{\mathbf{k}2\sigma})$ and $\psi^\dagger_{\mathbf{k}\mathcal{B}\sigma} = e^{-i\varphi_{\mathbf{k}}}(b^\dagger_{\mathbf{k}1\sigma}, b^\dagger_{\mathbf{k}2\sigma})$, where $\varphi_{\mathbf{k}} = \arg\{f_{\mathbf{k}}\}$. The Hamiltonian H_0 in this basis is

$$\hat{H}_{0\mathbf{k}} = -\begin{pmatrix} 0 & t_0 & t|f_{\mathbf{k}}| & 0 \\ t_0 & 0 & 0 & t|f_{\mathbf{k}}| \\ t|f_{\mathbf{k}}| & 0 & 0 & t_0 \\ 0 & t|f_{\mathbf{k}}| & t_0 & 0 \end{pmatrix}. \tag{5}$$

In mean field, the interaction operator $H_{\rm int}$, Eq. (3), is replaced by a single-particle operator which breaks a certain symmetry of the system. As shown in Ref. 13 the ground state of our model is G-type AFM (that is, the spins on any two nearest-neighbor sites are antiparallel), for which the spin-up and spin-down electron densities are redistributed as $n_{1\mathcal{A}\uparrow} = n_{2\mathcal{B}\uparrow} = n_{2\mathcal{A}\downarrow} = n_{1\mathcal{B}\downarrow} = (1 + x + \Delta n)/2$ and $n_{1\mathcal{A}\downarrow} = n_{2\mathcal{B}\downarrow} = n_{2\mathcal{A}\uparrow} = n_{1\mathcal{B}\uparrow} = (1 + x - \Delta n)/2$, while the total on-site electron density $n = n_{ia\sigma} + n_{ia\bar{\sigma}} = 1 + x$ is the same for any site. The mean-field interaction Hamiltonian for such phase is

$$H^{\rm MF}_{\rm int} = \frac{Ux}{2}\hat{N} + \Delta\sum_{\mathbf{k}}(\psi^\dagger_{\mathbf{k}\mathcal{A}\downarrow}\hat{\sigma}_z\psi_{\mathbf{k}\mathcal{A}\downarrow} - \psi^\dagger_{\mathbf{k}\mathcal{A}\uparrow}\hat{\sigma}_z\psi_{\mathbf{k}\mathcal{A}\uparrow} - \psi^\dagger_{\mathbf{k}\mathcal{B}\downarrow}\hat{\sigma}_z\psi_{\mathbf{k}\mathcal{B}\downarrow} + \psi^\dagger_{\mathbf{k}\mathcal{B}\uparrow}\hat{\sigma}_z\psi_{\mathbf{k}\mathcal{B}\uparrow}), \tag{6}$$

where $\hat{\sigma}_z$ is the Pauli matrix and $\Delta = U\Delta n/2$ is the AFM gap, which should be found self-consistently.

To find the gap, we solve the corresponding Shrödinger equation and derive the expressions for four electron bands $E^s(\mathbf{k})$ and eigenvectors $\upsilon^{(s)}_{ia\sigma\mathbf{k}}$

$$\begin{aligned} E^{(1,4)}_{\mathbf{k}} &= \mp\sqrt{\Delta^2 + (t\zeta_{\mathbf{k}} + t_0)^2}, \\ E^{(2,3)}_{\mathbf{k}} &= \mp\sqrt{\Delta^2 + (t\zeta_{\mathbf{k}} - t_0)^2}, \end{aligned} \tag{7}$$

where $\zeta_{\mathbf{k}} = |f_{\mathbf{k}}|$. In sublattice $\mathcal{A}$ for layer 1, the spin-up wave functions $\upsilon^{(s)}_{1\mathcal{A}\uparrow\mathbf{k}}$ are

$$\upsilon^{(s)}_{1\mathcal{A}\uparrow\mathbf{k}} = \tfrac{1}{2}\left[1 - \Delta/E^{(s)}_{\mathbf{k}}\right]^{1/2}. \tag{8}$$

The self-consistent equation for the gap is

$$n_{1\mathcal{A}\uparrow} = \frac{n}{2} + \frac{\Delta}{U} = \sum_{s=1}^{4}\int\frac{d\mathbf{k}}{V_{\rm BZ}}|\upsilon^{(s)}_{1\mathcal{A}\uparrow\mathbf{k}}|^2\Theta\left(\mu' - E^{(s)}_{\mathbf{k}}\right), \tag{9}$$

where $\mu' = \mu - Ux/2$, Θ is the Heaviside step function, and $V_{\rm BZ}$ is the volume of the Brillouin zone. The total number of electrons (per site) n is related to μ according to

$$n = \frac{1}{2}\sum_{s=1}^{4}\int\frac{d\mathbf{k}}{V_{\rm BZ}}\,\Theta\left(\mu' - E^{(s)}_{\mathbf{k}}\right). \tag{10}$$

At half-filling, $n = 1$, $x = 0$, and $\mu' = 0$. The lower two bands are filled while the upper two are empty. Upon electron doping, $x > 0$ (hole doping, $x < 0$), μ' abruptly changes to the new value $\mu' > \Delta$ ($\mu' < -\Delta$). Substituting the wave functions $\upsilon^{(s)}_{1\mathcal{A}\uparrow\mathbf{k}}$ into Eq. (9), one obtains

$$1 = \frac{U}{4t}\int_0^3 d\zeta\,\rho_0(\zeta)\left[\frac{1 - \Theta(|\mu'|/t - \sqrt{\delta^2 + (\zeta + \zeta_0)^2})}{\sqrt{\delta^2 + (\zeta + \zeta_0)^2}} + \frac{1 - \Theta(|\mu'|/t - \sqrt{\delta^2 + (\zeta - \zeta_0)^2})}{\sqrt{\delta^2 + (\zeta - \zeta_0)^2}}\right], \tag{11}$$

where $\delta = \Delta/t$, $\zeta_0 = t_0/t$, and $\rho_0(\zeta)$ is the dimensionless density of states $\rho_0(\zeta) = \int d\mathbf{k}\, \delta(\zeta - \zeta_\mathbf{k})/V_{BZ}$. Equation (10) implies

$$|x| = \frac{1}{2}\int_0^3 d\zeta\, \rho_0(\zeta)[\Theta(|\mu'|/t - \sqrt{\delta^2 + (\zeta + \zeta_0)^2}) + \Theta(|\mu'|/t - \sqrt{\delta^2 + (\zeta - \zeta_0)^2})]. \quad (12)$$

By solving Eqs. (11) and (12) we obtain $\Delta(x)$ and $\mu(x)$. This can be done analytically if $\Delta_0 \ll t, t_0$ (Δ_0 is the gap at zero doping). If Δ_0 is small, the value of $|\mu'| \sim \Delta_0$ is also small, and we can omit Θ-functions in the first terms in Eqs. (11) and (12). From these, we derive

$$2\rho_0(\zeta_0)\ln(\Delta_0/\Delta) \cong 2\rho_0(\zeta_0)\mathrm{asinh}(\delta\zeta/\delta),$$
$$|x| \cong \rho_0(\zeta_0)\delta\zeta, \quad (13)$$

where $\delta\zeta = \sqrt{(\mu')^2 - \Delta^2}/t$. By solving Eqs. (13), we obtain

$$\Delta = \Delta_0\sqrt{1 - |x|/x_c}, \quad (14)$$

$$\mu = \Delta_0[\mathrm{sgn}\,(x) - x/2x_c] + Ux/2, \quad (15)$$

where the critical doping $x_c \cong \Delta_0 t_0/\pi\sqrt{3}t^2$ (the analytical expression for Δ_0 in the limit $\Delta_0 \ll t, t_0$ was found in Ref. 13). We see from Eq. (14) that the value of the gap decreases with doping, and $\Delta = 0$, if $|x| \geqslant x_c$. The curves $\Delta(x)$ are symmetric for electron ($x > 0$) and hole ($x < 0$) doping. Next-nearest-neighbor hopping breaks this symmetry. However, for the parameters characteristic of graphene systems, the asymmetry of $\Delta(x)$ does not exceed 1–2%. The critical doping x_c as function of U is shown in Fig. 2. Strictly speaking, Eqs. (14) and (15) are not valid for $\Delta_0 \gtrsim t, t_0$. However, numerical calculations demonstrate that Eq. (14) holds true with very high accuracy for any ratio of Δ_0/t.

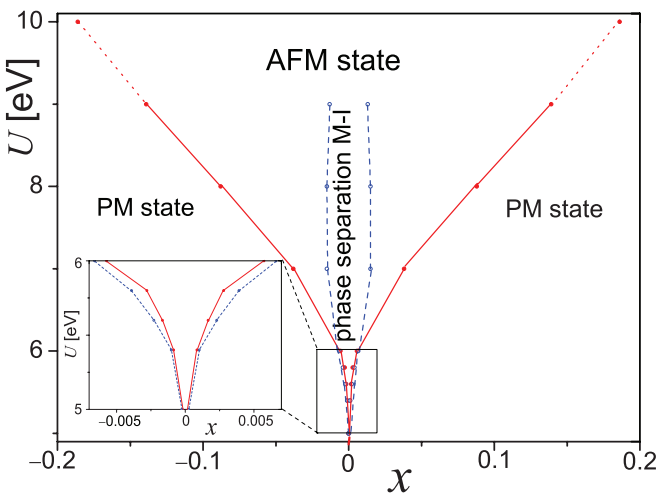

FIG. 2. (Color online) (x, U) phase diagram. Solid (red) lines show the boundary of the uniform AFM state x_c. For large U, our mean-field calculations are not quantitatively valid. To emphasize this, the dotted lines plot x_c for $U > 9$ eV. The dashed (blue) lines show the boundary of the phase-separated state. The inset shows the magnified phase diagram for 5 eV $< U <$ 6 eV.

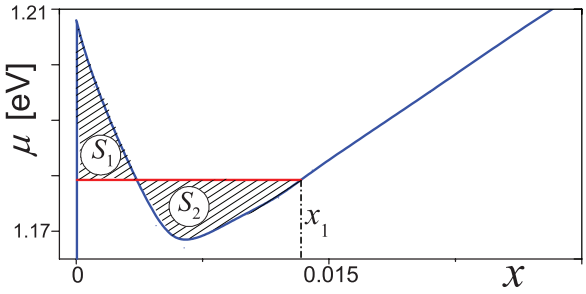

FIG. 3. (Color online) Chemical potential μ vs doping x for the homogeneous state, $U = 7$ eV [solid (blue) line]. The horizontal (red) line shows the Maxwell construction, shaded areas are equal: $S_1 = S_2$.

In addition to the usual AFM order parameter, more exotic possibilities are considered in the literature. For example, doping suppresses the AFM gap, inducing a canted state,[17] in which the angle between the magnetization vectors in different magnetic sublattices differs from 180°. However, our direct numerical calculations of the free energy show that such canted state is unstable for any doping. Furthermore, the doped AA-BLG is a typical system with imperfect nesting and, therefore, a helical AFM state can be induced in it.[18] This possibility is analyzed below.

Phase separation and metal-insulator transition. The chemical potential μ versus doping obtained from Eqs. (11) and (12) is shown in Fig. 3. Note that $\partial\mu/\partial x < 0$, if $|x|$ is small (this result does not depend on the sign of x). In particular, from Eq. (15) it follows that $\partial\mu/\partial x < 0$, if $U/t < \pi\sqrt{3}t/t_0$, which is valid for our choice of parameters. Thus, the compressibility $\kappa \sim \partial x/\partial\mu$ is negative, indicating the instability of the homogeneous phase toward phase separation upon doping. From Fig. 3, there are two stable phases with different doping: $x_0 = 0$ and $x_1 > 0$. The value of x_1 can be found using the Maxwell construction,[19] according to which the shaded areas in Fig. 3 are equal: $S_1 = S_2$. The calculated values of x_1 are shown by the (blue) dashed lines in Fig. 2 for different Us. For the case shown in Fig. 3, $x_1 < x_c$, and the uniform system separates into AFM insulator and AFM metal. For smaller U, the situation changes: $x_1 > x_c$, and the coexisting phases are AFM insulator and paramagnetic (PM) metal (see the inset in Fig. 2).

If the doped system were to remain uniform, even small doping would cause a transition from the insulating magnetic phase to a metallic phase, magnetic or not. However, the instability of the uniform phase and the ensuing phase separation delays the transition to the conducting phase until a finite critical concentration of dopants is reached. Because of this phase separation, the doped charge segregates into clusters inside the insulating AFM matrix. The precise structure of such phase depends on a variety of factors: impurities and defects in the sample or the substrate, the long-range Coulomb repulsion that arises due to local charge-neutrality breaking,[20] surface tension at the phase boundaries,[20,21] and electron-phonon interactions.[22] Charge conservation implies that the concentration p of the metallic phase is $p = |x|/x_1$. The percolative M-I transition occurs if p exceeds some threshold value p^*, which is usually about 0.5 for two-dimensional (2D) systems, and the corresponding threshold value of doping can be estimated as $|x^*| \sim 0.5\, x_1$.

Discussion. The most direct and controllable way to switch AA-BLG from AFM insulator to metal is doping the system with electron or holes, which could be attained by using appropriate dopants (e.g., NO_2,[3] Ca, K[23]), choosing the substrate and applying a gate voltage,[24,25] or combining these factors. Our analysis predicts that for interaction and hopping parameters values typical for graphene systems, phase separation exists in the doping range $0 < x < x_1$, where $x_1 \sim 0.5$–1.5%. Thus, the M-I transition occurs at $x^* \sim 0.25$–0.75%. For graphene systems, the doping levels $\sim 1\%$ are within the reach of current experimental techniques such as the adsorption of NO_2 gas molecules.[3,26] Moreover, even higher dopings, necessary to reach the van Hove singularity, were achieved.[23] These results suggest that the M-I transition we discuss in this paper can be realized experimentally.

As mentioned above, we did not include the helical AFM state in our considerations. Such simplification may be justified. Indeed, the helical AFM phase is mathematically equivalent to the Fulde-Ferrel-Larkin-Ovchinnikov (FFLO) state in superconductors,[27,28] which is very sensitive to disorder[29] and experimentally difficult to observe. Further, even if the helical state survives disorder, the phase separation and the M-I transition remain nonetheless: In such a situation the electrons segregate into insulating commensurate AFM and metallic helical phases[28,30] with the critical concentration x^* being slightly different from the values estimated above. At the same time, the mathematical description[18] of the helical AFM is fairly involved and cumbersome. Thus, we believe that at the present stage of this research our simplification of the M-I transition is warranted.

The above calculations are restricted to the mean field approximation. To what extent does the mean field theory offer a reliable description of the system? This question was discussed in Ref. 31 for the usual BCS model and for the BCS-like models with finite spin polarization in Refs. 32–34. It is generally agreed that for weak interaction the mean field calculations are accurate in these situations. In the intermediate-coupling regime the mean field results remain qualitatively correct. Since the superconducting systems investigated in these papers are mathematically equivalent to the AFM, both doped and undoped, we may conclude that our results are at least qualitatively correct even for moderately high U. Currently, numerical many-body approaches (functional renormalization group[35,36] and Monte Carlo[35,37]) demonstrated their usefulness for studies of monolayer and bilayer graphene. These methods may be used as alternatives to the mean field approach.

If we want to generalize the formalism for finite T, we must remember that in 2D at $T > 0$ no long-range AFM order exists. However, the short-range AFM order survives up to temperatures $T^*(x) \sim \Delta(x)$. Indeed, following the approach described in Refs. 13,38–40, we obtain the estimate of the crossover temperature in our model $T^*(x) \sim T_{\mathrm{MF}}(x) \approx 0.6\Delta(x)$, where $T_{\mathrm{MF}}(x)$ is the mean-field transition temperature.[40] Thus, the crossover temperature is higher than 100 K even if U is as small as 5 eV.

The phase separation can also be destroyed if the temperature exceeds a certain threshold value T_{PS}. To calculate T_{PS} we have to replace $1 - \Theta(\mu' - E_{\mathbf{k}})$ by $f(-E_{\mathbf{k}} - \mu') - f(E_{\mathbf{k}} - \mu')$ in Eq. (11) and Θ-functions by the Fermi distributions in Eq. (12) [$f(\varepsilon)$ is the Fermi distribution function]. Then, we derive $\mu = \mu(x,T)$ as a function of doping and temperature. If $T > T_{\mathrm{PS}}$, the function $\mu(x,T)$ increases monotonously with x. Our numerical analysis shows that $T_{\mathrm{PS}} \gtrsim 100$ K, if $U > 5.5$ eV.

In conclusion, antiferromagnetic order, a metal-insulator transition, and phase separation are predicted for the doped AA-stacked graphene bilayer. These effects can be observed at temperatures up to 100 K or even higher.

Acknowledgments. This work was supported in part by JSPS-RFBR Grant No. 12-02-92100, RFBR Grant No. 11-02-00708, ARO Grant-in-Aid for Scientific Research (S), MEXT Kakenhi on Quantum Cybernetics, and the JSPS via its FIRST program. A.O.S. acknowledges partial support from the Dynasty Foundation and RFBR Grant No. 12-02-31400.

[1] A. Rozhkov, G. Giavaras, Y. P. Bliokh, V. Freilikher, and F. Nori, Phys. Rep. **503**, 77 (2011).

[2] L. Zhang, Y. Zhang, M. Khodas, T. Valla, and I. A. Zaliznyak, Phys. Rev. Lett. **105**, 046804 (2010); A. Bostwick, J. L. McChesney, K. V. Emtsev, T. Seyller, K. Horn, S. D. Kevan, and E. Rotenberg, Phys. Rev. Lett. **103**, 056404 (2009).

[3] S. Y. Zhou, D. A. Siegel, A. V. Fedorov, and A. Lanzara, Phys. Rev. Lett. **101**, 086402 (2008).

[4] G. Kalon, Y. J. Shin, and H. Yang, Appl. Phys. Lett. **98**, 233108 (2011).

[5] J. B. Oostinga, H. B. Heersche, X. Liu, A. F. Morpurgo, and L. M. K. Vandersypen, Nat. Mater. **7**, 151 (2008).

[6] S. Adam, S. Cho, M. S. Fuhrer, and S. Das Sarma, Phys. Rev. Lett. **101**, 046404 (2008).

[7] Z. Liu, K. Suenaga, P. J. F. Harris, and S. Iijima, Phys. Rev. Lett. **102**, 015501 (2009).

[8] J. Borysiuk, J. Soltys, and J. Piechota, J. Appl. Phys. **109**, 093523 (2011).

[9] P. L. de Andres, R. Ramírez, and J. A. Vergés, Phys. Rev. B **77**, 045403 (2008).

[10] E. Prada, P. San-Jose, L. Brey, and H. Fertig, Solid State Commun. **151**, 1075 (2011).

[11] C. W. Chiu, S. H. Lee, S. C. Chen, F. L. Shyu, and M. F. Lin, New J. Phys. **12**, 083060 (2010).

[12] Y.-H. Ho, J.-Y. Wu, R.-B. Chen, Y.-H. Chiu, and M.-F. Lin, Appl. Phys. Lett. **97**, 101905 (2010).

[13] A. L. Rakhmanov, A. V. Rozhkov, A. O. Sboychakov, and F. Nori, Phys. Rev. Lett. **109**, 206801 (2012).

[14] J.-C. Charlier, J.-P. Michenaud, and X. Gonze, Phys. Rev. B **46**, 4531 (1992).

[15] L. Pisani, J. A. Chan, B. Montanari, and N. M. Harrison, Phys. Rev. B **75**, 064418 (2007); D. Soriano, N. Leconte, P. Ordejón, J.-C. Charlier, J.-J. Palacios, and S. Roche, Phys. Rev. Lett. **107**, 016602 (2011).

[16] T. O. Wehling, E. Şaşioğlu, C. Friedrich, A. I. Lichtenstein, M. I. Katsnelson, and S. Blügel, Phys. Rev. Lett. **106**, 236805 (2011); A. Du, Y. H. Ng, N. J. Bell, Z. Zhu, R. Amal, and S. C. Smith, J. Phys. Chem. Lett. **2**, 894 (2011).

[17] A. H. Morrish, *The Physical Principles of Magnetism* (IEEE Press, New York, 2001).

[18]T. M. Rice, Phys. Rev. B **2**, 3619 (1970).
[19]M. Le Bellac, F. Mortessagne, and G. G. Batrouni, *Equilibrium and Non-equilibrium Statistical Thermodynamics* (Cambridge University Press, Cambridge, 2004).
[20]J. Lorenzana, C. Castellani, and C. di Castro, Europhys. Lett. **57**, 704 (2002); R. Jamei, S. Kivelson, and B. Spivak, Phys. Rev. Lett. **94**, 056805 (2005); K. I. Kugel, A. L. Rakhmanov, and A. O. Sboychakov, *ibid*. **95**, 267210 (2005).
[21]A. L. Rakhmanov, A. V. Rozhkov, A. O. Sboychakov, and F. Nori, Phys. Rev. B **85**, 035408 (2012).
[22]K. I. Kugel, A. L. Rakhmanov, A. O. Sboychakov, N. Poccia, and A. Bianconi, Phys. Rev. B **78**, 165124 (2008).
[23]J. L. McChesney, A. Bostwick, T. Ohta, T. Seyller, K. Horn, J. González, and E. Rotenberg, Phys. Rev. Lett. **104**, 136803 (2010).
[24]T. J. Echtermeyer, L. Britnell, P. K. Jasnos, A. Lombardo, R. V. Gorbachev, A. N. Grigorenko, A. K. Geim, A. C. Ferrari, and K. S. Novoselov, Nat. Commun. **2**, 458 (2011).
[25]S. Kim, I. Jo, D. C. Dillen, D. A. Ferrer, B. Fallahazad, Z. Yao, S. K. Banerjee, and E. Tutuc, Phys. Rev. Lett. **108**, 116404 (2012).
[26]Y.-C. Lin, C.-Y. Lin, and P.-W. Chiu, Appl. Phys. Lett. **96**, 133110 (2010).
[27]P. Fulde and R. A. Ferrell, Phys. Rev. **135**, A550 (1964); A. I. Larkin and Yu. N. Ovchinnikov, Sov. Phys. JETP **20**, 762 (1965); L. G. Aslamazov, *ibid*. **28**, 773 (1969).
[28]D. E. Sheehy and L. Radzihovsky, Ann. Phys. **322**, 1790 (2007).
[29]S. Takada, Prog. Theor. Phys. **43**, 27 (1970).
[30]A. L. Rakhmanov, A. V. Rozhkov, A. O. Sboychakov, and F. Nori, Phys. Rev. B **87**, 075128 (2013).
[31]Š. Kos, A. J. Millis, and A. I. Larkin, Phys. Rev. B **70**, 214531 (2004).
[32]S. Pilati and S. Giorgini, Phys. Rev. Lett. **100**, 030401 (2008).
[33]F. Chevy, Phys. Rev. A **74**, 063628 (2006).
[34]A. Bulgac and M. McNeil Forbes, Phys. Rev. A **75**, 031605(R) (2007).
[35]T. C. Lang, Z. Y. Meng, M. M. Scherer, S. Uebelacker, F. F. Assaad, A. Muramatsu, C. Honerkamp, and S. Wessel, Phys. Rev. Lett. **109**, 126402 (2012).
[36]M. M. Scherer, S. Uebelacker, and C. Honerkamp, Phys. Rev. B **85**, 235408 (2012).
[37]J. E. Drut and T. A. Lähde, Phys. Rev. Lett. **102**, 026802 (2009); S. Hands and C. Strouthos, Phys. Rev. B **78**, 165423 (2008); P. V. Buividovich, E. V. Luschevskaya, O. V. Pavlovsky, M. I. Polikarpov, and M. V. Ulybyshev, *ibid*. **86**, 045107 (2012); P. V. Buividovich and M. I. Polikarpov, *ibid*. **86**, 245117 (2012).
[38]S. Chakravarty, B. I. Halperin, and D. R. Nelson, Phys. Rev. B **39**, 2344 (1989).
[39]E. Manousakis, Rev. Mod. Phys. **63**, 1 (1991).
[40]A. M. J. Schakel, *Boulevard of Broken Symmetries: Effective Field Theories of Condensed Matter* (World Scientific, Singapore, 2008).